A Study of the Dynamics and Control of the Model IV Fluidized Catalytic Cracking Process

Dhia Yasser Aqar

South Refineries Company, MoO/ Iraq

Abstract

Fluid catalytic cracking (FCC) is one of the most important chemical units in oil refineries due to its economic benefits. This research work concentrates on improving the control system of the Model IV FCC unit where dynamic modeling and the control ability based on the (McFarlane et al., 1993) model. Different open-loop tests were carried out in the wash oil flow rate (F_1) and the furnace fuel flow rate (F_5) to find the FCC models using Sundaresan and Krishnaswamy (S&K) and fraction incomplete response (FIR) methods. The riser temperature (T_r) and the regenerator bed temperature (T_g) were chosen as the control variables while (F_1 and F_5) were selected as the corresponding manipulated variables based on the relative gain array (RGA). PI controller tuning parameters were evaluated using the internal model control (IMC) method and different closed-loop control responses were examined for both set point tracking and disturbance rejection changes. Additional adjustments to the IMC filter constant were employed to further improve the closed loop responses for the system.

Keywords: FOPTD, FCCU, IMC, RGA, Multivariable, Decoupling

1. Introduction

Fluid catalytic cracking (FCC) is one of the key processes in the modern day petroleum industry. The main purpose of a FCC unit is to upgrade high-boiling, high-molecular weight hydrocarbon fractions of crude oil, and heavy distillates such as gas oil or residues to more valuable lighter products mainly gasoline, and lighter gases. The catalytic cracker is the key to profitability in that the successful process of the unit determines whether or not the refiner can stay competitive in today's market [1].

Many FCC models have been investigated relied on various mathematical dynamic modeling assumptions related to network cracking reactions; and composition hydrodynamics. Some studies have only concentrated on the regenerator section in their models while others have studied the reactor. Many works have included both the reactor and the regenerator together. Lee and Groves [2] developed a mathematical model of the fluidized bed catalytic cracking plant to give a description of the regenerator by assuming it as a simple stirred tank with a dense bed phase. But this model lacks detailed kinetics for the combustion of carbon monoxide and carbon dioxide that takes place in two regions of regenerator: solid part of catalytic surface and the homogeneous phase part. Lee and Groves proposed the three lumps model in the reactor (riser) section. McFarlane et al. [12] developed a dynamic simulator (Model IV) for the reactor-regenerator system and auxiliary equipment (feed preheater, air lift blower, and wet gas compressor, etc.). This model described the dynamics of the catalyst circulation rate in FCC unit and the interactions between the outputs constrained variables such as the regenerator and the reactor. Cristea et al. [3] improved a new dynamic FCC model as a modern control theory based on the McFarlane et al. model for side-by- side FCC unit, assuming a bubbling-bed regenerator runs in the partial combustion (coke does not completely burn to CO_2 and CO). Alsabei [4] developed model IV depended on McFarlane et al. and Cristea et al. with a five-lump model. It is covered the subsystems of reactor- regenerator, the main fractionator modeling. These features were able to solve the gasoline and diesel yields and estimating the impact of input initial conditions on the output variables. Many studies have been published about the relative gain array (RGA) method that is used for selection of suitable pairings between the output control variables and the manipulated variables. Hovd and Skogestad [5] proposed a completed selection of best coupling control system study of a FCC unit. Their work relied on a linear model generated from nonlinear model of Lee and Groves. Fernandes [6] presented the appropriate loop pairings for both 2x2 and 4x4 control systems. Ramachandran [7] developed the use of statistical analysis to predict the temperature riser dynamics in order to reduce the nonlinear system variability and maximizing gasoline productivity. Therefore, the aims of the present study are to develop a new mathematical model and to select the best possible pairing.

2. Analytical Mathematical Model of the FCC Unit

Figure (1) shows the description of a FCC unit [8]. The nonlinear model, along with steady state parameter values, is given below by McFarlane et al [12]. The model captures the major dynamic effects that happen in an actual FCC unit .It is multivariable, highly nonlinear system, several constrained variables and cross coupling interaction loops between input and output variables. McFarlane et al. [12] provided an extensive mathematical dynamic model, which was integrated into the Simulink program for this proposed work. The McFarlane model covered the six major parts of the entire FCC unit: (1) Feed and preheated system (2) reactor (riser and stripper) (3) main fractionator column and wet gas compressor machine (4) regenerator (5) air combustion blowers (6) catalyst circulation lines.

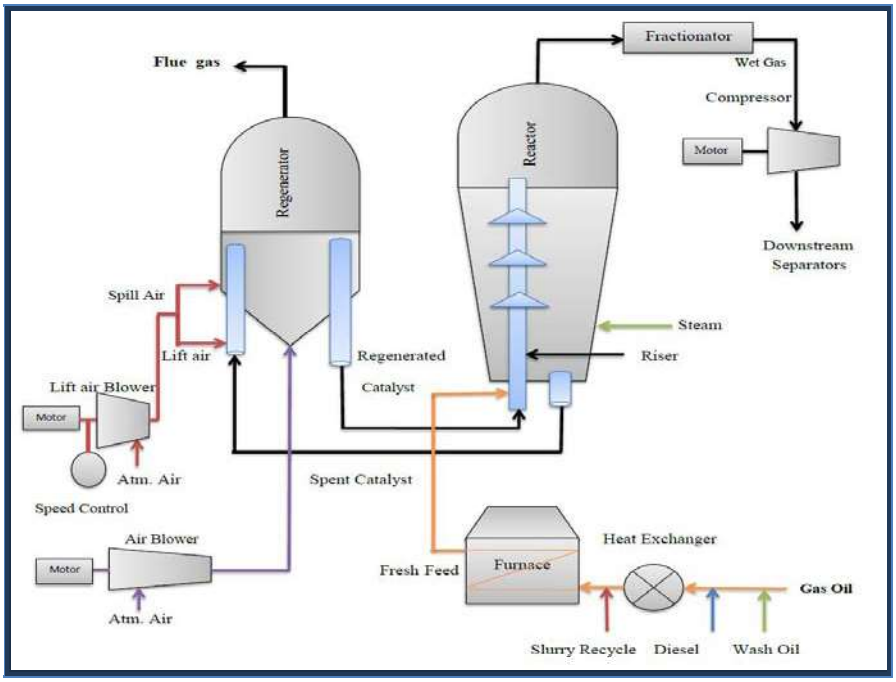

Fig. (1) Process Diagram of FCC Unit.

Figure (2) illustrates Simulink block diagram, which was utilizes for dynamic modeling and control purposes. This Matlab Simulink program used and modified depended on the McFarlane et al. model was originally developed by Emad Ali from King Saud University [9]. The model ran in the simulator uses the Matlab differential algebraic equation solver (ode45) with a simulation time equal to 1500 minutes. The ode45 functions are used to solve the spatial ordinary differential equations for the regenerator. More details are shown in Appendix A as presented completely at McFarlane et al. model.

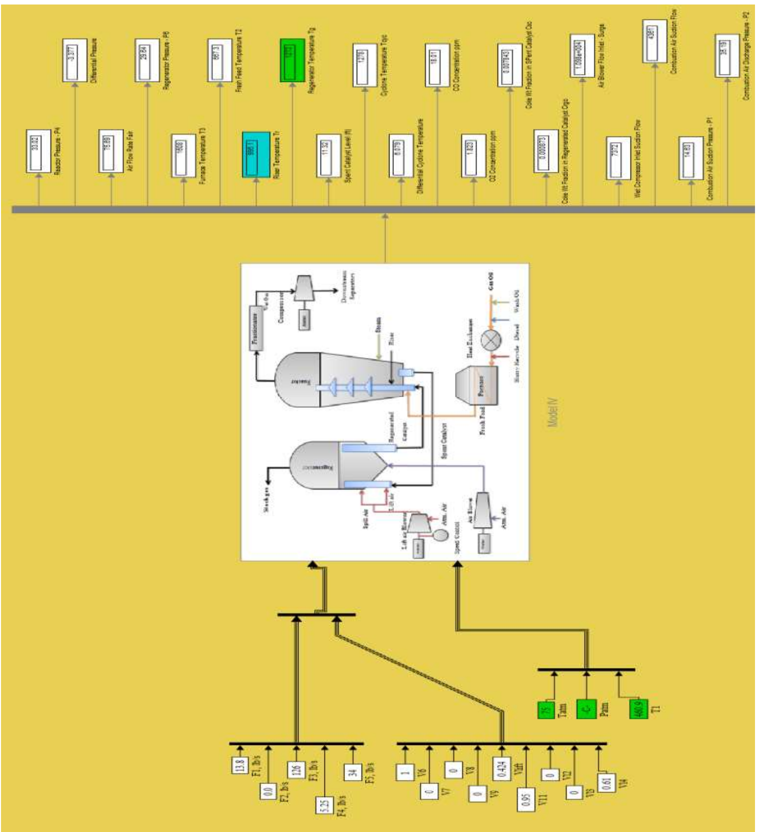

Fig. (2) Simulink Program for Open-Loop Simulation

3- Results and Discussion

3.1 FCC Process Variables

Several output variables which can be regulated in an FCC unit. For the proposed FCC process, the riser temperature (T_r), the regenerator temperature (T_g), and the level spend catalyst in standpipe (L_{sp}) were tested for control purposes. These control variables are all impacted by many input variables such as the wash oil flow rate (F_1), the recycle oil flow rate (F_4), and the flow rate of fuel to the furnace (F_5). For instance, when the step values of F_4 decrease, the final output variables values (i.e. T_r, T_g, and L_{sp}) also decrease. If the step values of F4 are increased, the final output values (i.e. T_r, T_g, and L_{sp}) increase. Figure (3) shows how the output variables (i.e. T_r, T_g, and L_{sp}) magnitude changes as a function of changing magnitude in the input variables (i.e. F_4). These plots illustrate the nonlinearity of the process which if were a linear system would have no curvature.

Figure (3) is result from different magnitudes in step size from the nominal base case value of F4 equal to 5.25 lb/s. The curves in this figure are caused by various magnitudes in step size from the initial steady state values. The process gain (K) in a positive direction is not equal to the gain in a negative direction for the nonlinear model in open-loop examination. On other hand, the linear model has the same values of the process gain at both directions.

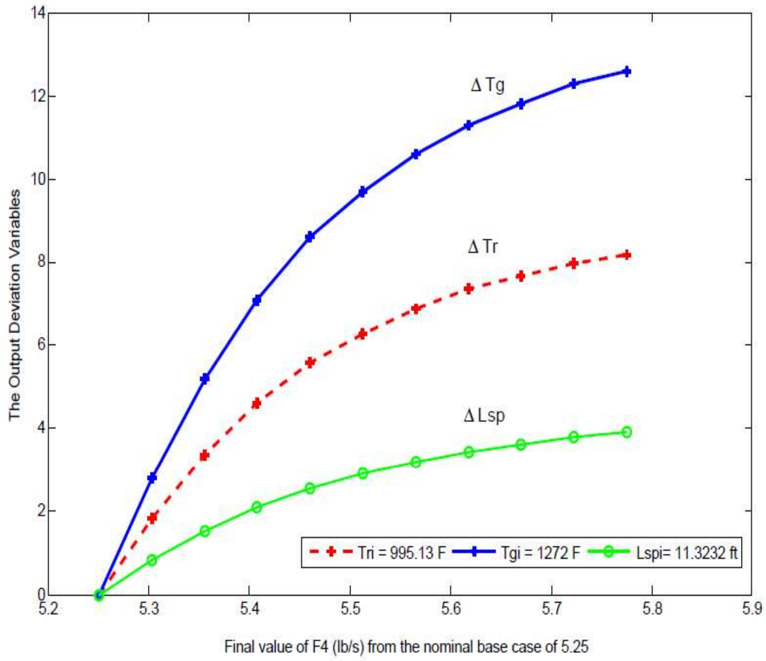

Fig. (3) Operating values of ΔTr, ΔTg, and ΔLsp as a function of increasing recycled oil flow rate

Figure (4) illustrates how the steady state gain (K) (defined as the ratio of output change over input change) varies as a function of the magnitude of the step size in manipulated variable (i.e. ΔF_4), and the effect of the initial step values on the process gain. As presented in figure (4), as the final value of F_4 is decreased from the initial value of 5.25 lb/s, all final values of gain relating T_r decrease which indicates a reduced gain and hence nonlinear behavior. Figure (4) shows that the K1, K2 systems are nonlinear and that the K3 system is approximately linear. The process gains (K1, K2 and K3) are simply the steady state change in the riser temperature (ΔT_{rj}) to the size of the input step change (ΔF_4) at the different steady state values of F_4. ΔF_4 means that the difference between the new step change and the initial steady state of F_4. As ΔF_4 decreases, K decreases for all 3 sets of data. More plots of K values versus the positive and negative values of the other manipulated variables (ΔF_1 and ΔF_5) illustrate a same behavior, and are not presented in this work.

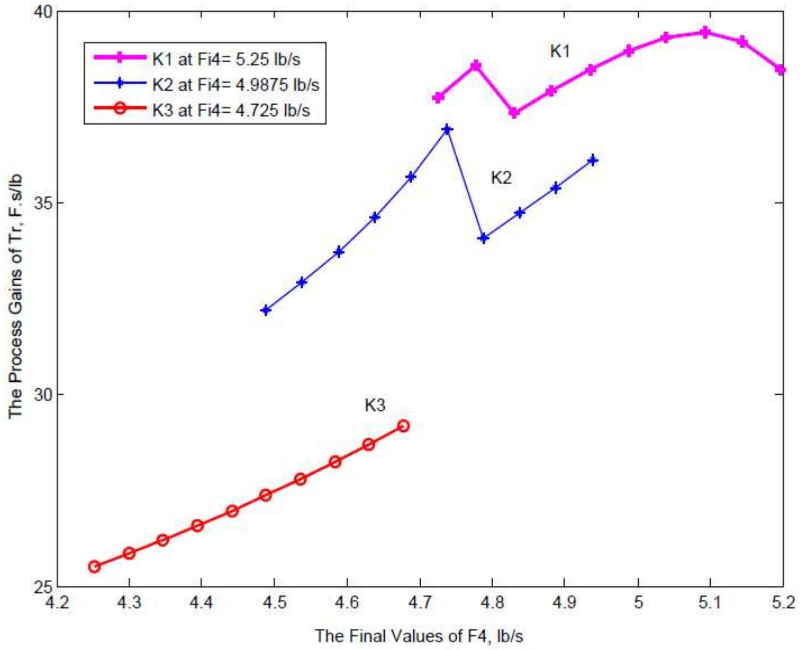

Fig. (4) The process gains of Tr against the negative final values of F4

3.2 The FCC Models Estimation Fitting to the Simulator Data

The FOPTD models of the FCC process parameters were basically evaluated from the FIR method and the S&K method (see tables 3&4). The generated FCC models were matched to data from the Simulator using the Simulink software for data generation. Several step tests were implemented in F_1 and F_5, respectively. All step tests in F_1 and F_5 were positive, and each step test has a different magnitude (i.e. +1, 5, and 10%). Figure (5) shows the curve fitting of the FOPTD transfer function to the Simulator data in different step changes in F_5. It can be observed from this following figure that the all FOPTD models are good fits to the Simulator (McFarlane et al. data) data.

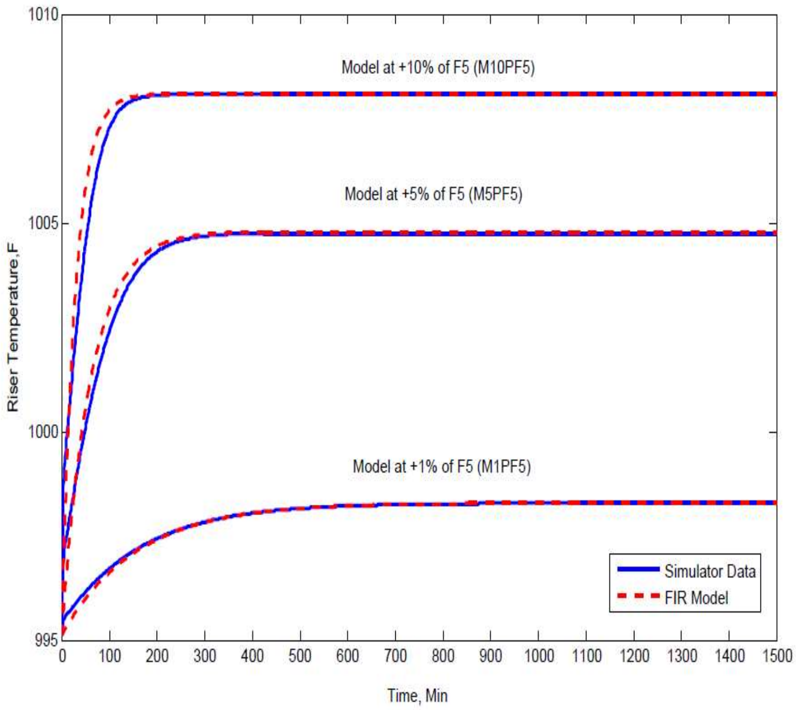

Fig. (5) Fitting of simulator data to generation model at various step changes

3.3 Selection of the Best Control Loops Scheme Based on RGA

Bristol's approach of the relative gain array (RGA) is one of the first important ways for measuring process interactions based on steady state initial conditions [10]. The main goal of RGA is to choose the most important pairing of the controlled and manipulated variables in order to reduce the degree of interaction between control loops. The relative gain can be estimated from the following dimensionless ratio of open-loop gain to closed-loop gain at steady state operation conditions [11]:

$$\lambda_{ij} = \frac{\text{open - loop gain}}{\text{closed - loop gain}} \qquad (1)$$

When the sign of λ_{ij} is negative, the closed-loop and open-loop parings run in the opposite direction and must be avoided to prevent providing an unstable process.

$$RGA = \begin{pmatrix} \lambda_{11} & \lambda_{12} \\ \lambda_{21} & \lambda_{22} \end{pmatrix} \qquad (2)$$

T_r, T_g, and L_{sp} were selected first to be the output variables, and the input variables as F_5, F_1, F_4 and a RGA scheme was performed for this work. It can be drown from this selection that the appropriate coupling of a RGA matrix for a 3x3 system leads to a higher condition number (CN) for all cases by pairing (T_r) loop with F_5 and (T_g) loop with F_1, and (L_{sp}) loop with F_4 in order to avoid a negative sign of RGA main diagonal element matrix. These CN values clearly indicate a poorly conditioned process. So, a 3x3 control scheme was reduced to a 2x3 control system by removed one of three output variables. The two output variables (T_r and T_g) were paired with three input variables (F1, F4, F5) respectively as a non-square RGA analysis for a 2x3 control system. Depended on their having small CN and acceptable values of λ (close to unity), the pairings of (T_r- F_5) and (T_g- F_1) show to be the most promising ones, for the proposed FCC process, riser reactor temperature (T_r) and regenerator temperature (T_g) are assumed as controlled variables and furnace fuel flow rate (F_5) and wash oil flow rate (F_1) are the corresponding manipulated variables. Table (1) illustrates two output variables (T_r, T_g) with two input variables (F_1, F_5) as a square RGA analysis. This table shows that different relative gain values are created from different step changes in F_1 and F_5, as would be expected from a nonlinear process (see Tables 3&4). The table also gives the possible paring between the input variables and output variables, and the condition number for a Matrix (CN). CN is the ratio of the largest to the smallest nonzero singular values of a matrix. When CN is larger than 10, the system will be difficult to control (ill conditioned), while a well-conditioned system has a CN below 10. The singular values (σ) are positive numbers as the nonnegative square roots of the eigenvalues of steady state gain matrix. The condition number also gives powerful information about the sensitivity of the matrix properties to changes in the matrices elements. CN and σ can be easily computed using Matlab for matrix analysis.

Table (1) RGA Matrixes of Several 2x2 Control Scheme Pairing

Step Change	K	λ	CN	The Possible Pairing	K_{New}	λ_{New}
+1%	$\begin{bmatrix} 21.0855 & 9.3024 \\ 32.6087 & 12.3529 \end{bmatrix}$	$\begin{bmatrix} -6.0758 & 7.0758 \\ 7.0758 & -6.0758 \end{bmatrix}$	40.73	$\begin{bmatrix} Tr-F5 & Tr-F1 \\ Tg-F5 & Tg-F1 \end{bmatrix}$	$\begin{bmatrix} 9.3024 & 21.0855 \\ 12.3529 & 32.6087 \end{bmatrix}$	$\begin{bmatrix} 7.0758 & -6.0758 \\ -6.0758 & 7.0758 \end{bmatrix}$
-1%	$\begin{bmatrix} 24.4696 & 10.9268 \\ 39.13 & 15.2941 \end{bmatrix}$	$\begin{bmatrix} -7.0176 & 8.0176 \\ 8.0176 & -7.0176 \end{bmatrix}$	46.5	$\begin{bmatrix} Tr-F5 & Tr-F1 \\ Tg-F5 & Tg-F1 \end{bmatrix}$	$\begin{bmatrix} 10.9268 & 24.4696 \\ 15.2941 & 39.13 \end{bmatrix}$	$\begin{bmatrix} 8.0176 & -7.0176 \\ -7.0176 & 8.0176 \end{bmatrix}$
+5%	$\begin{bmatrix} 11.9855 & 5.6882 \\ 18.2609 & 6.8235 \end{bmatrix}$	$\begin{bmatrix} -3.7025 & 4.7025 \\ 4.7025 & -3.7025 \end{bmatrix}$	25.13	$\begin{bmatrix} Tr-F5 & Tr-F1 \\ Tg-F5 & Tg-F1 \end{bmatrix}$	$\begin{bmatrix} 5.6882 & 11.9855 \\ 6.8235 & 18.2609 \end{bmatrix}$	$\begin{bmatrix} 4.7025 & -3.7025 \\ -3.7025 & 4.7025 \end{bmatrix}$
-5%	$\begin{bmatrix} 23.2186 & 11.4998 \\ 37.8261 & 16.7647 \end{bmatrix}$	$\begin{bmatrix} -8.5099 & 9.5099 \\ 9.5099 & -8.5099 \end{bmatrix}$	52	$\begin{bmatrix} Tr-F5 & Tr-F1 \\ Tg-F5 & Tg-F1 \end{bmatrix}$	$\begin{bmatrix} 11.4998 & 23.2186 \\ 16.7647 & 37.8261 \end{bmatrix}$	$\begin{bmatrix} 9.5099 & -8.5099 \\ -8.5099 & 9.5099 \end{bmatrix}$
+10%	$\begin{bmatrix} 7.2246 & 3.8147 \\ 11.0145 & 4.0294 \end{bmatrix}$	$\begin{bmatrix} -2.2556 & 3.2556 \\ 3.2556 & -2.2556 \end{bmatrix}$	15.7	$\begin{bmatrix} Tr-F5 & Tr-F1 \\ Tg-F5 & Tg-F1 \end{bmatrix}$	$\begin{bmatrix} 3.8147 & 7.2246 \\ 4.0294 & 11.0145 \end{bmatrix}$	$\begin{bmatrix} 3.2556 & -2.2556 \\ -2.2556 & 3.2556 \end{bmatrix}$
-10%	$\begin{bmatrix} 20.8242 & 10.2945 \\ 35.0725 & 15.3235 \end{bmatrix}$	$\begin{bmatrix} -7.6063 & 8.6063 \\ 8.6063 & -7.6063 \end{bmatrix}$	47.76	$\begin{bmatrix} Tr-F5 & Tr-F1 \\ Tg-F5 & Tg-F1 \end{bmatrix}$	$\begin{bmatrix} 10.2945 & 20.8242 \\ 15.3235 & 35.0725 \end{bmatrix}$	$\begin{bmatrix} 8.6063 & -7.6063 \\ -7.6063 & 8.6063 \end{bmatrix}$

3.4 Internal Model Control (IMC)

There are more comprehensive model-based design ways for tuning controllers. The most important method is Internal Model Control (IMC) [13] which allows model uncertainty and tradeoffs the closed-loop system performance against process robustness. IMC tuning for PI controllers is used for this work. The PI controller values based on IMC tuning K_C and τ_i, and also λ (a filter parameter amounts to the desirable feedback time constant) are estimated from table (2).

For this work a model using FOPTD transfer function model may be written as:

$$G(s) = \frac{K}{\tau s+1} e^{-td} \qquad (3)$$

Table (2) IMC Approximate Model Controller Tuning Rules

PI controller Form	K_C	τ_i	Recommended Choice of λ ($\lambda > 0.2\tau$ always)
$G_{(s)} = K_c\left(1 + \frac{1}{\tau_i s}\right)$	$K_C = \frac{2\tau+td}{2K(\lambda+td)}$	$\tau_i = \tau + \frac{td}{2}$	$\frac{\lambda}{td} > 1.7$

The controller gain (K_c), and the reset time (τ_i) are considered very important to achieving a desired regulatory approach. The S&K and FIR methods were used to find the first order plus time delay (FOPTD) model parameters of T_r, and T_g that are derived from positive and negative step changes in F_1 & F_5, as presented in tables (3&4).

Table (3) FCC unit Model Parameters of Tr for ± Step Changes in F5 (G11)

Step Change (scf/s)	K (^{0}F.s/ scf)	τ (Min)	td (Min)
+1%	9.3	156	0
+5%	5.7	60.6	10.2
+10%	3.8	28.8	10.4
-1%	10.9	199.5	0
-5%	11.5	236.5	6.2
-10%	10.3	156.7	6

Table (4) FCC unit Model Parameters of Tg for ± Step Changes in F1 (G22)

Step Change (lb/s)	K (^{0}F.s/ lb)	τ (Min)	td (Min)
+1%	32.6	158	7.6
+5%	18.3	65.7	15.3
+10%	11	36.2	12.7
-1%	39.1	213.7	4.9
-5%	37.8	182.9	9.4
-10%	35.1	155.4	13.6

The best selected FCC models tested for control purposes (set point and disturbance changes) are M10PF1, and M10PF5, as shown in table (5). The models (M10PF1 and M10PF5) are called for +10% step changes in (F_1 & F_5) from tables 3&4. The main concept of these FCC model values of the PI controllers selections were relied on a smaller controller gain values and a smaller CN (see tables 1, 3&4) to assure stability and maximize productivity.

Table (5) PI Controller Tuning Parameters

FCCU Model	Kc	τ_i (Min)
M10PF1	0.18	42.52
M10PF5	0.504	33.97

4. Simulink Program Discussion

Figure (6) illustrates Simulink program of two feedback controllers controlling T_r, and T_g. Different closed loop responses tests were proceeded on the FCC system and the results are explained below. It shows the Simulink interface and how the two feedback controllers are connected to the modeling equations which are written in Matlab. This figure was discussed previously in section 2.

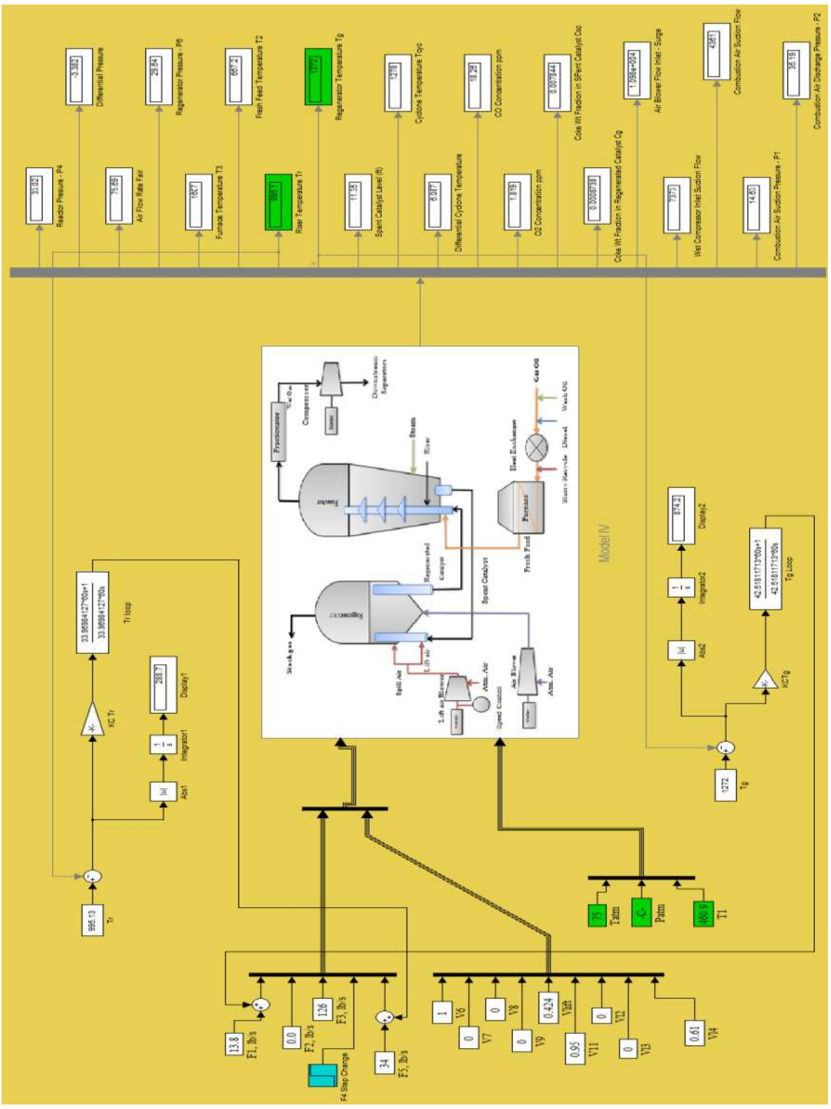

Fig. (6) Performing Two PI Controllers for Tr, and Tg Loops

4.1 The Controlled Variables Responses to Set Point Change

Figures (7.a &7.b) show the closed loop responses for both T_r and T_g to a +2% increase in the T_r set point tracking change which was performed over a period of 1500 minutes. It can be realized that the closed-loop performances with the feedback controllers depended on model M10PF1 for T_g and M10PF5 for T_r

performed well, and have a quick response for both T_r and T_g to the desired operation set points.

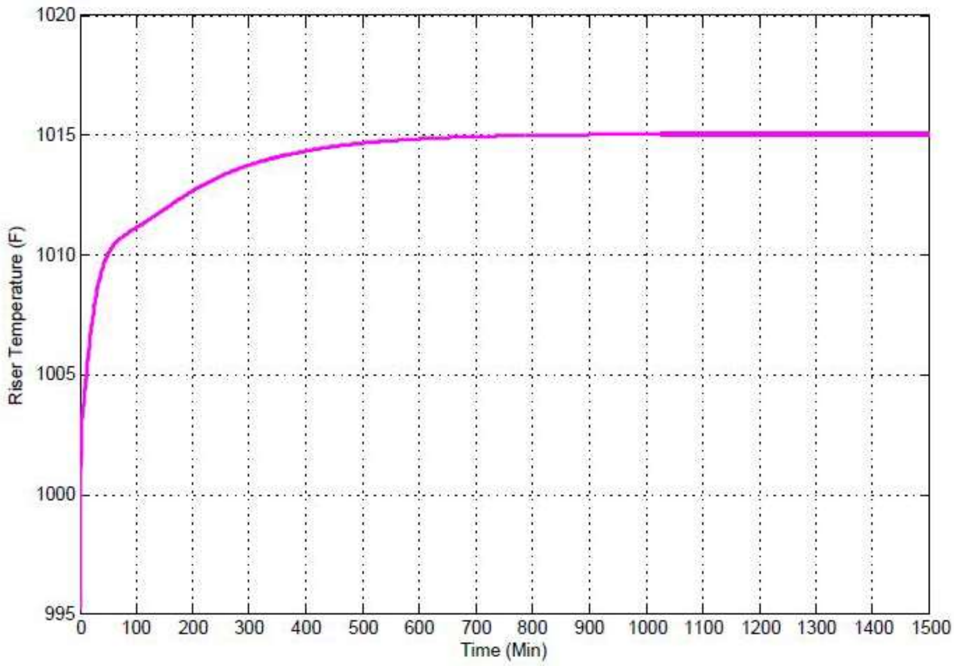

Fig. (7.a) The Closed Loop Response of Tr to +2% Tr set point

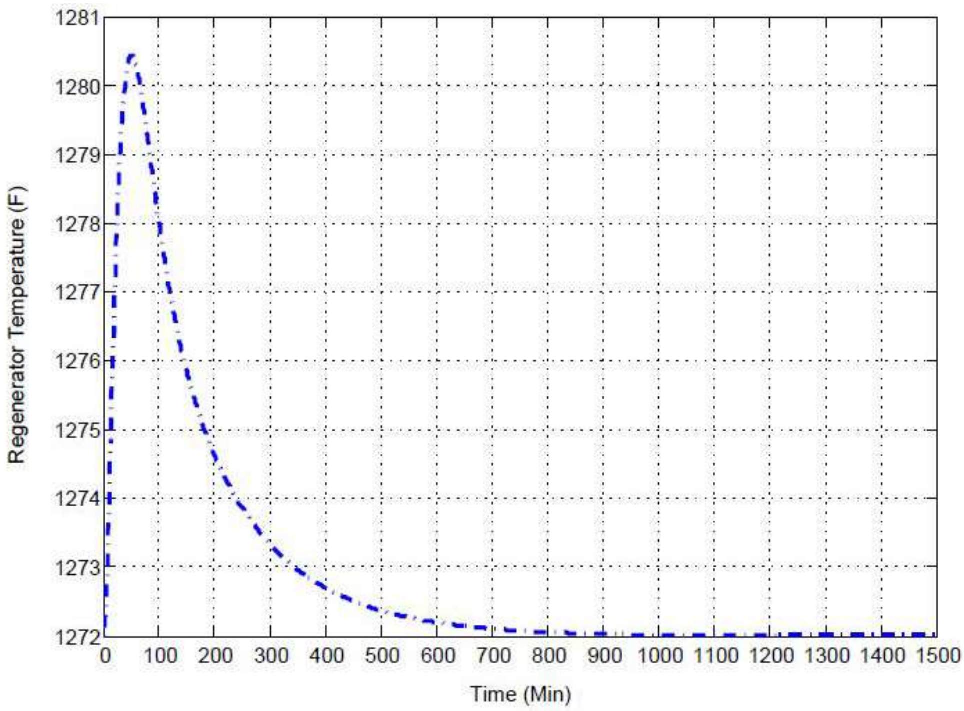

Fig. (7.b) The Closed Loop Response of Tg to +2% Tr set point

4.2 The Controlled Variables Responses to Feed Disturbance Change

In the case of the disturbance problem scenario, it is assumed the +2% increase in the flow of fresh feed to reactor riser (F_3), figures (8.a &8.b) show the closed-loop dynamic system performances of the two controlled variables (T_r and T_g). As noticed from this figures, the closed-loop responses of (M10PF1 and M10PF5) for T_r, T_g to the disturbance change respond quickly. To prove that the responses of models (M10PF1, M10PF5) for T_r, T_g have the best values the Integral of the Absolute Value (IAE) method.

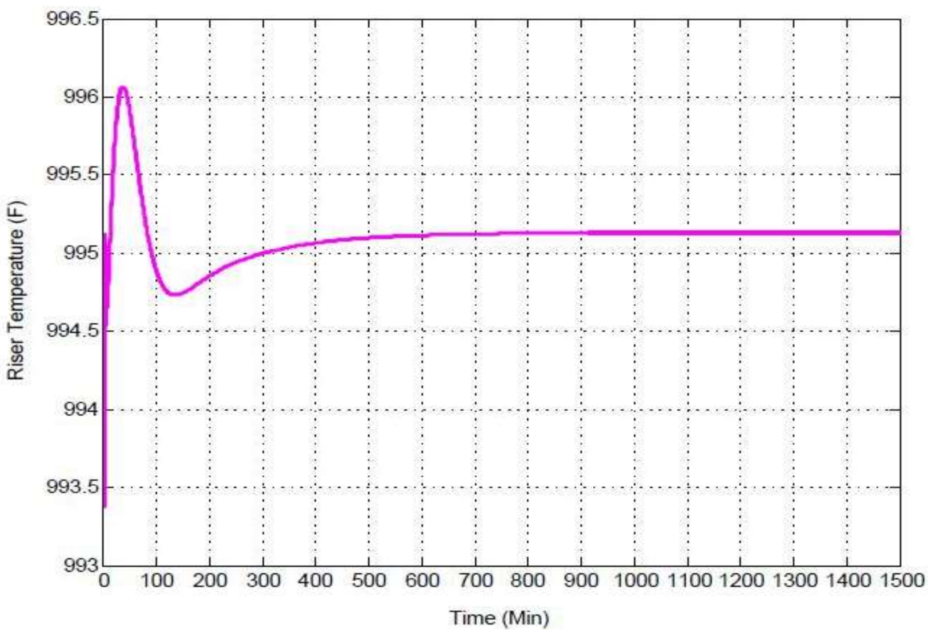

Fig. (8.a) The Closed Loop Response of Tr to +2% of F_3

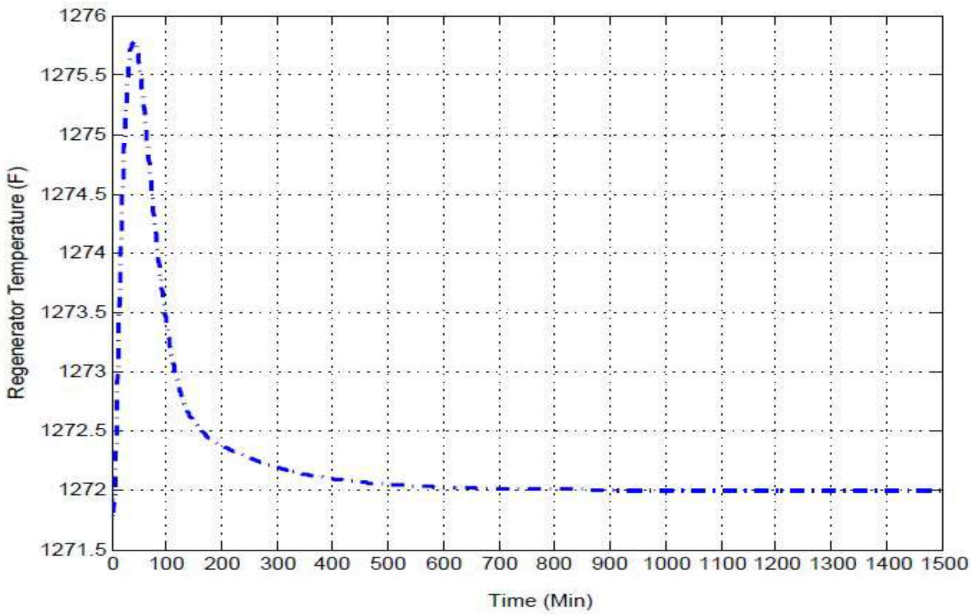

Fig. (8.b) The Closed Loop Response of Tg to +2% of F_3

5. The IMC Filter Parameters (λ) Modification

To improve SISO of PI controller system performances, the M10PF1 parameters in table 5 were selected. The filter parameter (λ) of T_g was only used for the adjustment approach to disturbance changes in Temperature of fresh feed entering furnace (T_1). K_c is a function of the filter parameter (λ). When the filter parameter (λ) is adjusted, the value of K_c changes (see tables 2&6). The filter parameter (λ) value is 21.55 minute. The IAE method in the Simulink program was used to estimate the PI controller performances. The IAE performance index is determined using the following form [14]:

$$IAE=\int_0^{\infty} |e\ (t)|\ dt \qquad (4)$$

Where, e (t) is the error of the loop signal that can be defined as the deviation between the set point values and measured variable. The fresh feed temperature (T_1) was ramped up and down by 3.94^0C over 600 second, and there is no ramp function change effect of T_g loop on T_r loop, as given in figure (9) and table (6). When T_1 ramp change was made, the regenerator temperature reached the original set point. But the riser temperature achieved the new operating steady state of 535 ^{0}C. A comparison between the (λ = 21.55) and (λ = 8, 4, 2) responses of T_g shows that the response of (λ = 2) has the best response based on the IAE criteria however the response is oscillatory. As a consequence a value of (λ= 4) is preferred since it has good performance with minimal oscillations. The main idea of presenting controller transfer functions at each process loop (G_{CTr}, and G_{CTg}) in the plots is to verify that the controller process respond differently direction from the output controlled variables loops. Also, it can be concluded that (λ) value modifies in the T_r loop have no interaction loop impact on the T_g loop.

Table (6) IAE Performance Analysis of the Tg Loop to +8.5% of T1 Disturbance at Simulation Time = 300 min

Study Case	λ	Kc	IAE Index at Positive Step Change in T_1 in T_r Loop	IAE Index at Positive Step Change in T_1 in T_g Loop
Case A1	21.55	0.18	2.84E+04	1.95E+04
Case A2	8	0.488	2.88E+04	8.61E+03
Case A3	4	0.97	2.90E+04	4.47E+03
Case A4	2	1.93	2.91E+04	2.28E+03

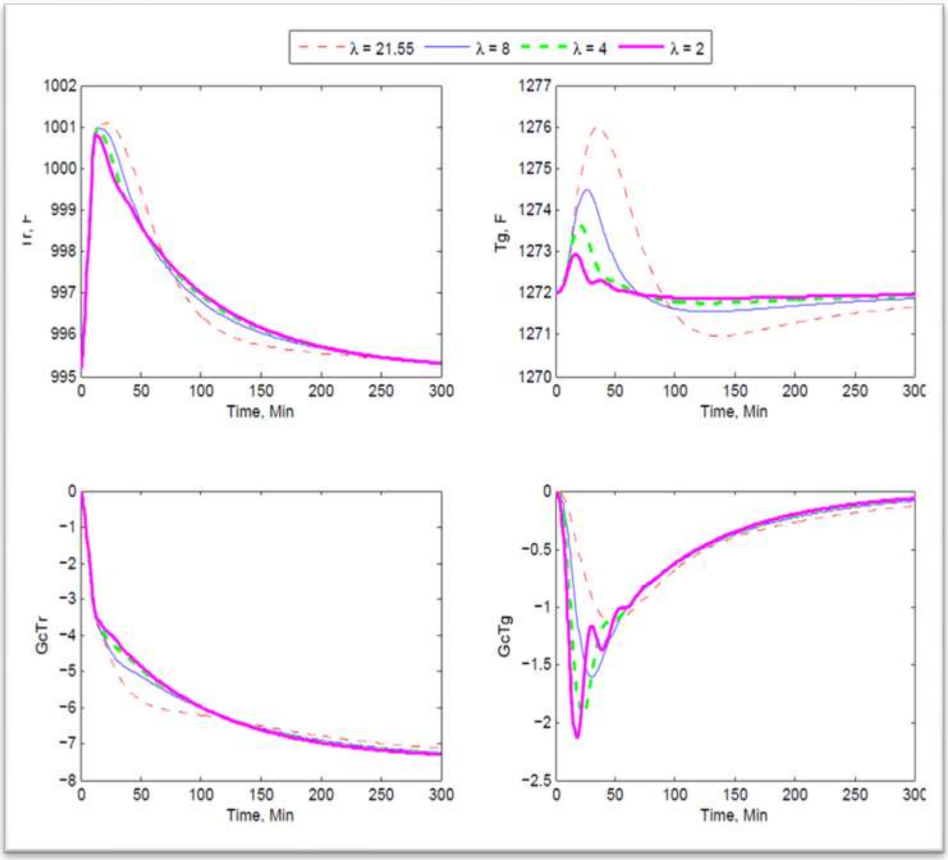

Fig. (9) Comparison of the Various Filter Parameters (λ) Values in Tg Loop at +8.5% increases in T_1

Finally, the closed-loop system responses of very small filter parameters (λ) did not perform well as compared to the bigger (λ) values responses for feed input disturbances changes. The closed-loop responses of proposed controlled variables at negative feed disturbance changes were not shown because they gave the same results as the positive disturbance changes. Figure (10) shows the selected filter parameter responses of (λ = 3.5) at both negative and positive directions of ± 8.5% increase in T_1. These selections were based on the good control responses and lower IAE values. These can lead to the increase of productivity of the FCC unit; can minimize time consumption and the interaction process loops.

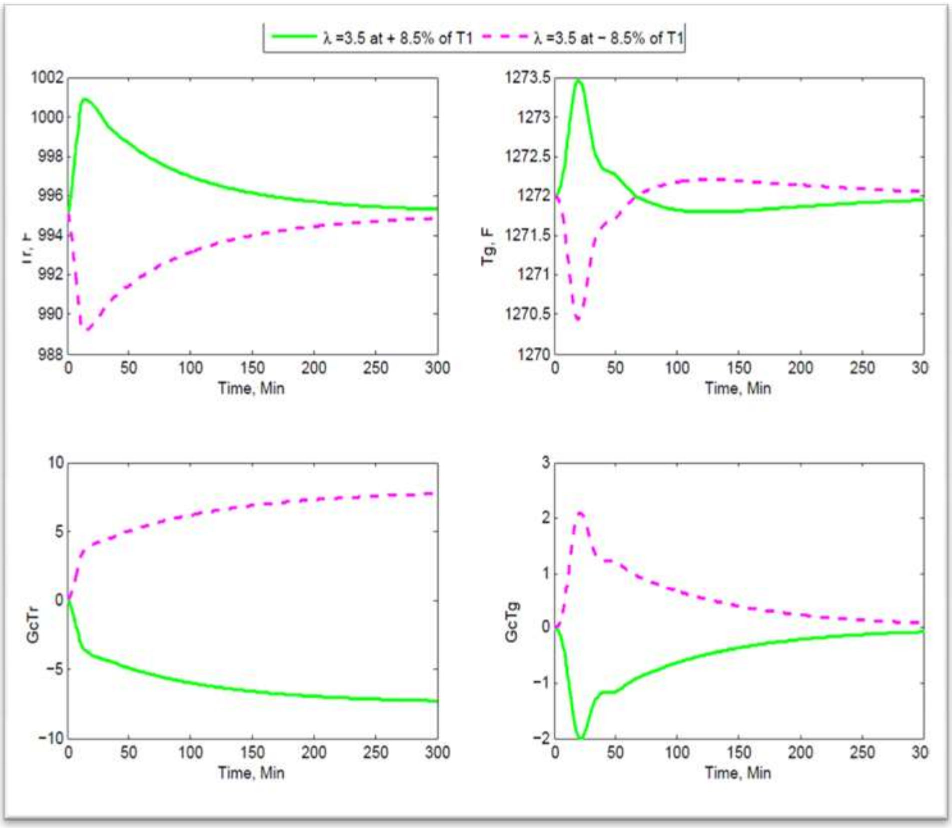

Fig. (10) The selected filter parameters (λ) value in Tg loop at ± 8.5% in T_1

5. Conclusion

According to the results gathered from this work, several important conclusions can be drawn. First of all, the FCC unit is obviously presented as a nonlinear process with different dynamic modeling behaviors. Linear PI controllers for T_r, and T_g were derived from the nonlinear process through the use of a set of linear models that can be used to describe the process dynamic behavior. The closed-loop performance of the controllers based on M10PF1and M10PF5 models outperformed the others model based controllers for both set point and feed disturbance changes. It can be also noticed that the PI controller responses are ultimately able to reject the disturbances. This technique however needs a significant long time to obtain the desired set points. In addition, the performance of the closed-loop system was improved when the filter parameter value (λ) was changed to optimize performance.

Nomenclature

Symbol	State Variable Description
A_{lp}	Cross sectional area of lift pipe (8.73 ft^2)
c_{pc}	Heat capacity of catalyst (0.31 Btu/mol ^{0}F)
C_g	Weight fraction of coke regenerated catalyst (lb Coke/lb Catalyst)
C_{sc}	Weight fraction of coke on spent catalyst (lb Coke/lb Catalyst)
F_{air}	Air flow rate into regenerator (mol/s)
F_{coke}	Production of coke in reactor riser (lb/s)
F_H	Burning rate of hydrogen (lb/s)
f_g	Force exerted by regenerated catalyst (lbf)
F_g	Flow rate of regenerated catalyst (lb/s)
F_{sc}	Flow rate of spent catalyst (lb/s)
F_{sp}	Flow into standpipe (lb/s)
F_{V6}	Flow through combustion air blower suction valve V_6 (lb/s)
F_{V7}	Flow through combustion air blower valve (lb/s)
F_{V8}	Flow through lift air blower vent valve (lb/s)
F_{V11}	Flow through wet gas compressor suction valve (mol/s)
F_{V12}	Flow through wet gas flare valve (mol/s)
F_{V13}	Flow through wet gas compressor anti-surge valve (mol/s)
F_{wg}	Wet gas production in reactor (mol/s)
F_4	Flow of slurry to reactor riser (lb/s)
F_5	Flow of fuel to furnace (scf/s)
F_6	Combustion air blower throughput (lb/s)
F_7	Combustion air flow to the regenerator (lb/s)
F_8	Lift air blower throughput (lb/s)
F_9	Lift air flow to the regenerator (lb/s)
F_{10}	Spill air flow to the regenerator (lb/s)
F_{11}	Wet gas flow to the vapor recovery unit (mol/s)
h_{ris}	Height of reactor riser (60 ft)
MCP_{eff}	Effective heat capacity of riser vessel and catalyst (10000Btu/^{0}F)
M_I	Effective heat capacity of regenerator mass (200,000Btu/^{0}F)
M_g	Inertial mass of regenerated catalyst (2 lb_f. s^2/ft)
n	Quantity of gas (mol)
P_{rb}	Pressure at bottom of reactor riser (psi)
P_1	Combustion air blower suction pressure (psi)
P_2	Combustion air blower discharge pressure (psi)
P_3	Lift air blower discharge pressure (psi)
P_4	Reactor pressure (psi)
	Reactor fractionator pressure (psi)

P_5	Regenerator pressure (psi)
P_6	Wet gas compressor suction pressure (psi)
P_7	Enthalpy into regenerator, reactor (Btu/s)
Q_{in}	Enthalpy out of regenerator, reactor (Btu/s)
Q_{out}	Heat loss from furnace (Btu/s)
Q_{Loss}	Universal gas constant (10.73 ft^3 psi/lbmol°R)
R	Time (s)
t	Atmospheric temperature (75°F)
T_{atm}	Combustion air blower discharge temperature (190°F)
$T_{comb,d}$	Lift air blower discharge temperature (225°F)
$T_{lift,d}$	Furnace log mean temperature difference (°F)
T_{lm}	Temperature of reactor riser (°F)
T_r	Temperature of regenerator bed (°F)
T_g	Temperature of fresh feed entering reactor riser (°F)
T_2	Steady state furnace outlet temperature (°F)
$T_{2,ss}$	Furnace firebox temperature (°F)
T_3	Furnace overall heat transfer coefficient (25 Btu/s)
UA_f	Combustion air blower discharge system volume (1000 ft^3)
$V_{comb,d}$	Combustion air blower suction system volume (200 ft)
$V_{comb,s}$	Lift air blower discharge system volume (200 ft^3)
$V_{lift,d}$	Regenerator volume occupied by gas (ft^3)
$V_{g,g}$	Velocity of regenerated catalyst (ft/s)
v_g	Inventory of carbon in regenerator (lb)
W_c	Inventory of catalyst in reactor (lb)
W_r	Inventory of catalyst in regenerator (lb)
W_g	Inventory of catalyst in regenerator standpipe (lb)
W_{sp}	Molar ratio of CO to air in stack gas (mol CO/mol air)
$X_{co,sg}$	Molar ratio of CO_2 to air in stack gas (mol CO/mol air)
$X_{CO2,sg}$	Heat of combustion of furnace fuel (1000 Btu/scf)
ΔH_{fu}	Density of air at regenerator conditions (lb/ft^3)
ρ_{airg}	Density of catalyst in lift pipe (lb/ft^3)
ρ_{lift}	Settled density of catalyst (68 lb/ft^3)
ρ_{part}	Average density of material in reactor riser (lb/ft^3)
ρ_{ris}	Furnace firebox time constant (200s)
τ_{fb}	Riser fill time (40s)
τ_{fill}	Furnace time constant (60s)
τ_{fo}	

Appendix A:

A.1. Feed and the preheated system

$$\frac{dT3}{dt} = (F_5\,\Delta H_{fu} - UA_f\,T_{lm} - Q_{Loss})\,/\tau_{fb} \quad \text{.............................. (1)}$$

$$\frac{dT2}{dt} = (T_{2,\,SS} - T_2)\,/\tau_{fo} \quad \text{... (2)}$$

A.2. Reactor model and coke and wet gas yield models

$$\frac{dC_{sc}}{dt} = \left\{F_g C_g + F_{coke} - F_{sc} C_{sc} - C_{sc}\frac{dW_r}{dt}\right\}\frac{1}{W_r} \quad \text{............................ (3)}$$

The catalyst balance is given by

$$\frac{dW_r}{dt} = F_g - F_{sc} \quad \text{...(4)}$$

Reactor riser energy balance is given by

$$MCP_{eff}\,\frac{dT_r}{dt} = Q_{in} - Q_{out} \quad \text{.. (5)}$$

Reactor riser pressure balance is given by

$$P_{rb} = P_4 + \frac{\rho_{ris} h_{ris}}{144} \quad \text{... (6)}$$

Reactor and main fractionator pressure balances is given by

$$\frac{dP_5}{dt} = 0.833(F_{wg} - F_{v_{11}} - F_{v_{12}} - F_{v_{13}}) \quad \text{....................... (7)}$$

$$\frac{dP_7}{dt} = 5(Fv_{11} - F_{11}) \quad \text{...(8)}$$

A.3. Regenerator model

$$[(W_g + W_{sp})\,C_{pc} + M_I]\,\frac{dT_g}{dt} = Q_{in} - Q_{out} \quad \text{.......................... (9)}$$

Carbon balance is given by

$$\frac{dC_g}{dt} = \left(\frac{dW_c}{dt} - C_g\frac{dW_g}{dt}\right)\frac{1}{W_g} \quad \text{. .... (10)}$$

$$\frac{dW_g}{dt} = F_{sc} - F_{sp} \quad \text{.......................... (11)}$$

$$\frac{dW_c}{dt} = (F_{sc}C_{sc} - F_H) - (F_{sp}C_g + 12F_{air}(X_{CO,sg} + X_{CO_2,sg})) \quad \text{....... (12)}$$

Standpipe inventory balance is given by

$$\frac{dW_{sp}}{dt} = F_{sp}\text{-}F_g \qquad \text{......................(13)}$$

Pressure balance is given by

$$\frac{dP_6}{dt} = \frac{1}{V_{g,g}}\left\{R\left(n\frac{dT_g}{dt} + (T_g+459.6)\frac{dn}{dt}\right)\right\} \text{....................} \quad (14)$$

Air lift calculations

$$\frac{d\rho_{lift}}{dt} = \left(\frac{F_{sc}}{v_{cat,lift}A_{lp}} + \rho_{airg} - \rho_{lift}\right)\frac{1}{\tau_{fill}} \qquad \text{..............................} \ (15)$$

A.4 Air blower

A.4.1 Combustion air blower

$$\frac{dP_1}{dt} = \frac{R\ (T_{atm}+459.6)}{29V_{comb,s}}\left(F_{V6}\text{-}F_6\right) = 0 \qquad \text{...............................} \ (16)$$

$$\frac{dP_2}{dt} = \frac{R\left(T_{comb,d}+459.6\right)}{29V_{comb,d}}\left(F_6\text{-}F_{V7}\text{-}F_7\right) \qquad \text{.............................} \ (17)$$

A.4.2 Lift air blower

$$\frac{dP_3}{dt} = \frac{R\left(T_{lift,d}+459.6\right)}{29V_{lift,d}}\left(F_8\text{-}F_{V8}\text{-}F_9\text{-}F_{10}\right) \qquad \text{.....................} \ (18)$$

A.5 Catalyst circulation

$$\frac{dv_g}{dt} = \frac{f_g}{M_g} = 0 \qquad \text{..} \ (19)$$

Appendix B: The input variables of the FCC unit model

State Variable Description	Symbol	Initial Condition
Wash oil flow set point	F_1^{set}	13.8 lb/s
Diesel flow rate set point	F_2^{set}	0 lb/s
Fresh feed rate set point	F_3^{set}	126 lb/s
Flow rate of Slurry recycle set point	F_4^{set}	5.25 lb/s
Fuel flow rate to the furnace	F_5^{set}	34 scf/s
Combustion air blower suction valve	V_6	1
Combustion air blower suction vent valve	V_7	0
Lift air blower suction vent valve position	V_8	0
Wet gas compressor suction valve position	V_9	0
Wet gas compressor suction vent valve	V_{11}	95%
Flue gas valve position	V_{12}	0
Lift air blower steam valve	V_{13}	0
Temperature of fresh feed entering furnace	V_{14}	61%
Atmospheric temperature	V_{lift}	42.4%
Atmospheric pressure	T_1	460.9 ^{0}F
	T_{atm}	75 ^{0}F
	P_{atm}	14.7 Psi

Appendix C: The steady state of the FCC unit model variables

State Variable Description	Symbol	Initial Condition
Regenerator temperature	T_g	1272 ^{0}F
Regenerator catalyst inventory	W_g	273742.7 lb
Regenerator carbon inventory	W_c	1297.62 lb
Weight fraction of coke on regenerated	C_g	8.7296 x 10^{-4} lb
Regenerator standpipe catalyst inventory	W_{sp}	3566.8 lb
Regenerator pressure	P_6	29.64 Psi
Catalyst density in the lift pipe	ρ_{lift}	3.251 lb / ft^3
Combustion Air blower section pressure	P_1	14.63 Psi
Combustion Air blower discharge pressure	P_2	35.19 Psi
Lift Air blower discharge pressure	P_3	40.5 Psi
Reactor riser temperature	T_r	995.13 ^{0}F
Weight fraction of coke on spent catalyst	C_{sc}	7.8432 x 10^{-3} lb
Reactor catalyst inventory	W_r	101359.4 lb
Reactor fractionator pressure	P_5	23.52 Psi
Wet gas compressor suction pressure	P_7	22.68 Psi
Fresh feed temperature	T_2	667.26 ^{0}F
Furnace firebox temperature	T_3	1607.55 ^{0}F
Quantity of gas	n	245.92 Mole

References

1. Reza Sadeghbeigi; "Fluid Catalytic Cracking Handbook", Second Edition, Gulf Publishing Company (2000).
2. Lee E. and Groves F. R.; "Mathematical Model of the Fluidized Bed Catalytic Cracking Plant", Trans. Soc. Comput. Simulation Pages 219-23 (1985).
3. Cristea M. V., Agachi P. S., Marinoiu V.; "Simulation and Model Predictive Control of a UOP Fluid Catalytic Cracking Unit", Chem. Eng. Process., 42 67 (2003).
4. Alsabe Redah Mousa; "Model Based Approach for the Plant-Wide Economic Control of Fluid Catalytic Cracking Unit', Ph.D. Dissertation, Loughborough University, (2011).
5. Hovd M, Skogestad S.; "Procedure for Regulatory Control Structure Selection with Application to the FCC Process", AIChE J. 1993, 39, 1938.
6. Fernandes J. L.; "Nonlinear Modeling of Industrial Fluid Catalytic Cracking Processes for Model-Based Control and Optimization Studies", Ph.D. Thesis, Institute Superior Tecnico, (2007).
7. Ramachandran R., Rangaiah G. P., Lakshminarayanan S.;"Data Analysis, Modeling and Control Performance Enhancement of an Industrial Fluid Catalytic Cracking Unit". Chem. Eng. Sci. 2007, 62, 1958.
8. Mythily M., Manamalli D., Manikandan P.; "Dynamic Modeling, Simulation and Multivariable Control Strategy Applied To Catalytic Cracking Unit", (2011).
9. Emad Ali; "Simulink Module. File from Internet: http://faculty.ksu.edu.sa/Emad.Ali/Pages/SimulinkModule.aspx(2012).
10. Bristol, E.H. On a new measure of interactions for multivariable process control. IEEE Trans. Autom. Control, AC-11:133-134 (1966).
11. Pandimadevi G., Indumathi P., Selvakumar V., Chemical Engineering Research & Volume 81, issue 7A, Pages 875-880(2010).

12. McFarlane R.C., Reineman R.C., Bartee J.F., Georgakis C.; “Dynamic simulator for a Model IV Fluid Catalytic Cracking Unit, Computers Chemical Engineering, 17(3):275-300 (1993).
13. Al-Mutairi Sultan Awadh; “The Use of Adaptive Multiple Model Control for a Nonlinear Distillation Process”. M.Sc. Thesis, Florida Institute of Technology, (2001).
14. Seborg D. E., Edgar T. F., Mellichamp D. A.; "Process Dynamics and Control", 2nd Edition, John Wiley and Sons, Inc., (2011).